

# Solitons and lumps in the cylindrical Kadomtsev–Petviashvili equation. I. Axisymmetric solitons and their stability

Cite as: Chaos 34, 013138 (2024); doi: 10.1063/5.0175696

Submitted: 8 September 2023 · Accepted: 27 November 2023 ·

Published Online: 25 January 2024







View Online



Export Citation



CrossMark

Wencheng Hu,<sup>1</sup>  Zhao Zhang,<sup>2</sup>  Qi Guo,<sup>2,a)</sup>  and Yury Stepanyants<sup>3,4,a)</sup> 

## AFFILIATIONS

<sup>1</sup>School of Physics and Optoelectronic Engineering, Zhongyuan University of Technology, Zhengzhou 450007, China

<sup>2</sup>Guangdong Provincial Key Laboratory of Nanophotonic Functional Materials and Devices, South China Normal University, Guangzhou 510631, People's Republic of China

<sup>3</sup>School of Mathematics, Physics and Computing, University of Southern Queensland, Toowoomba, QLD 4350, Australia

<sup>4</sup>Department of Applied Mathematics, Nizhny Novgorod State Technical University, n.a. R.E. Alekseev, 24 Minin St., Nizhny Novgorod 603950, Russia

<sup>a)</sup>Authors to whom correspondence should be addressed: [guoq@scnu.edu.cn](mailto:guoq@scnu.edu.cn) and [Yury.Stepanyants@usq.edu.au](mailto:Yury.Stepanyants@usq.edu.au)

## ABSTRACT

We revise soliton and lump solutions described by the cylindrical Kadomtsev–Petviashvili (cKP) equation and construct new exact solutions relevant to physical observation. In the first part of this study, we consider basically axisymmetric waves described by the cylindrical Korteweg–de Vries equation and analyze approximate and exact solutions to this equation. Then, we consider the stability of the axisymmetric solitons with respect to the azimuthal perturbations and suggest a criterion of soliton instability. The results of our numerical modeling confirm the suggested criterion and reveal lump emergence in the course of the development of the modulation instability of ring solitons in the unstable case. In the next part of this study, which will follow shortly, we will present exact solutions to the cKP equation describing weakly nonlinear waves in media with positive dispersion subject to the modulation instability of solitons with respect to small azimuthal perturbations.

Published under an exclusive license by AIP Publishing. <https://doi.org/10.1063/5.0175696>

Nonlinear waves in cylindrical geometry are a subject of interest in physics and mathematics due to their applied importance in the description of natural phenomena and their laboratory analogs, as well as due to the unusual structure of governing model equations and their solutions. The governing equations for weakly nonlinear waves in dispersive media, viz., the cylindrical Korteweg–de Vries (cKdV) equation and the cylindrical Kadomtsev–Petviashvili (cKP) equation (alias the Johnson equation), were derived by various authors since 1959. Particularly, approximate and even exact solutions have been obtained; however, there are some misinterpretations of solutions in physical variables that have not been critically assessed so far. In this study, which consists of two parts, we revise solitary-type solutions described by the cKdV and cKP equations and construct new exact solutions relevant to physical observations. In the first part of this study, we consider basically axisymmetric

waves described by the cKdV equation and analyze approximate and exact solutions of this equation. Then, we consider the stability of the axisymmetric solitons with respect to the azimuthal perturbations and suggest a criterion of soliton instability. The results of our numerical modeling confirm the suggested criterion and reveal lump emergence in the course of the development of the modulation instability of ring solitons in the unstable case. In the next part of this study, which will follow shortly, we will present exact solutions to the cKP1 equation describing weakly nonlinear waves in media with positive dispersion. Solitary waves with circular fronts in such media are subject to modulation instability with respect to small azimuthal perturbations. We will study the development of instability, the emergence of lumps (stable two-dimensional solitary waves), as well as interactions of periodic lump chains with each other and with ring solitons.

## I. INTRODUCTION

Cylindrical and quasi-cylindrical waves often appear in media with small nonlinearity and weak dispersion; see, for example, satellite images of internal waves generated by tides in the Mediterranean Sea near Gibraltar<sup>1</sup> and images of internal waves in the Cod Cape Bay, USA.<sup>2</sup> Such waves can be described by the cylindrical version of the Kadomtsev–Petviashvili (cKP) equation, known also as the Johnson equation. This equation in physical coordinates reads as

$$\frac{\partial}{\partial t} \left( \frac{\partial u}{\partial r} + \frac{1}{c} \frac{\partial u}{\partial t} - \frac{\alpha}{c} u \frac{\partial u}{\partial t} - \frac{\beta}{2c^5} \frac{\partial^3 u}{\partial t^3} + \frac{u}{2r} \right) = \frac{c}{2r^2} \frac{\partial^2 u}{\partial \varphi^2}, \quad (1.1)$$

where  $u(t, r, \varphi)$  is a wave perturbation that depends on time  $t$  and two spatial coordinates in the cylindrical coordinate frame  $(r, \varphi)$ ,  $c$  is the speed of long linear waves, and  $\alpha$  and  $\beta$  are the coefficient of nonlinearity and dispersion, respectively, which depend on parameters of a particular physical problem. The equation similar to Eq. (1.1) was derived for the first time for surface water waves in a shallow basin by Johnson<sup>3</sup> (see also Refs. 4–6 and 31), and then, for internal waves by Lipovskii,<sup>7</sup> and for plasma waves by Peng *et al.*<sup>8</sup> In the Appendix, we briefly reproduce the derivation of this equation for a general case when long nonlinear waves are described by the two-dimensional Boussinesq equation. In the derivation of Eq. (1.1), it was assumed that the wavefront is far from the center of the coordinate frame so that the last term in brackets is of the same magnitude of smallness as the nonlinear and dispersive terms. It was also assumed that the variation of a wavefront along the azimuthal variable  $\varphi$  is smooth so that the characteristic length of variation along  $\varphi$  is much greater than the length of a wavefront along  $r$ .

Note that the coefficient  $c > 0$  is the speed of long waves of infinitesimal amplitude; the coefficient  $\alpha$  can be of either sign; its sign only controls the polarity of a wave but does not have any influence on the wave shape or wave stability with respect to the azimuthal perturbations. In contrast to that, the sign of the coefficient  $\beta$  plays an important role both in the view of the wave shape and its stability. If we have an exact solution  $u_c(r, \varphi, t)$  to Eq. (1.1) with  $\beta > 0$  describing the outgoing ring wave, then the same solution but with the inverse polarity  $-u_c(r, \varphi, t)$  can be obtained for an incoming wave with  $\beta < 0$  and vice versa. Indeed, if we replace  $\beta \rightarrow -\beta$ ,  $c \rightarrow -c$ , and  $u \rightarrow -u$ , we obtain almost the same equation (1.1) but with the opposite sign of the coefficients in front of the second term and in front of the term on the right-hand side. Such an equation describes an incoming wave. However, the rear part of a nonsymmetric outgoing wave becomes under the transformation of the frontal part of an incoming wave. In addition to that, circular waves in media with the “anomalous dispersion,” i.e., with  $\beta < 0$ , are unstable with respect to the azimuthal perturbations, whereas, in media with the “normal dispersion,” i.e., with  $\beta > 0$ , they are stable. This issue is discussed below in detail.

To construct solutions to the cKP equation, it is convenient to reduce it to the widely used dimensionless “standard form” (see, for example, Ref. 9),

$$\frac{\partial}{\partial \tau} \left( \frac{\partial U}{\partial r} + 6U \frac{\partial U}{\partial \tau} + \frac{\partial^3 U}{\partial \tau^3} + \frac{U}{2r} \right) = -\sigma^2 \frac{3}{r^2} \frac{\partial^2 U}{\partial \theta^2}, \quad (1.2)$$

$$\text{where } r = r, \quad \tau = c^2 \left( \frac{2}{\beta c} \right)^{1/3} \left( \frac{r}{c} - t \right), \quad \theta = \varphi \sqrt{6c\sigma^2 \left( \frac{2}{\beta c} \right)^{1/3}},$$

$$U = \frac{\alpha u c}{6} \left( \frac{2}{\beta c} \right)^{1/3}. \quad (1.3)$$

Here, the parameter  $\sigma^2 = \pm 1$  determines the type of the cKP equation; its sign is the same as the sign of the dispersion parameter  $\beta$ ; therefore,  $\beta\sigma^2 > 0$ . The case with  $\sigma^2 = -1$  pertains to the cKP1 equation, which is applicable, in particular, to waves in a magnetized plasma,<sup>10,11</sup> waves in solids and on elastic plates,<sup>12</sup> oceanic internal waves in shear flows,<sup>13,14</sup> shallow-water waves with vertical odd viscosity,<sup>15</sup> etc., whereas the case with  $\sigma^2 = 1$  pertains to the cKP2 equation that describes, in particular, the surface or internal waves in shallow water<sup>16</sup> (see also the Appendix), waves in pair-ion-electron plasma.<sup>17</sup> Such a classification based on the parameter  $\sigma^2$  is very similar to the classification of the conventional quasi-one-dimensional KP equation (see, for example, Refs. 18 and 19).

If function  $U$  does not depend on  $\theta$ , then Eq. (1.2) reduces to the cylindrical Korteweg–de Vries (cKdV) equation, and the latter reduces to the plane KdV equation if a wavefront is straight. (Note that the cKdV equation was derived for the first time for surface water waves by Iordansky;<sup>20</sup> then, it was re-derived independently for water waves by A. A. Lugovtsov and B. A. Lugovtsov;<sup>21</sup> and then it was derived for plasma waves by Maxon and Viccelli;<sup>22</sup> see also Refs. 3, 7, 23, 52, 56, 58, and 59.) All four equations (KdV, cKdV, KP, and cKP) are completely integrable (there is also a relative elliptic KP equation, which is completely integrable too<sup>24</sup>). The representation of all these equations, except the classical KdV equation, in terms of Lax pairs of operators was established by Dryuma.<sup>25–27</sup> Various links between four relative equations were found by various authors<sup>3,4,21,28–30</sup> and summarized in Ref. 32 (see the diagram in Fig. 1). One-way arrows stand for that all solutions of one-dimensional equations KdV and cKdV can be transformed into some particular solutions of two-dimensional equations cKP and KP, respectively, by means of the relevant transformation. Two-way arrows stand for that there is one-to-one conformity between solutions of the corresponding equations, for example, between the KdV and cKdV or KP and cKP.

Using the links between these equations, one can formally derive solutions of the cKP equation from the other three equations, but not all of these solutions can be of physical meaning. New solutions to the cKP equation from the solutions of the KP equation were formally generated by many authors.<sup>9,17,33–36</sup> Some other formal solutions to the cKP equation were constructed by different methods in Refs. 8 and 37–39. We call these solutions formal because they do not satisfy the periodicity condition on the azimuthal variable  $\theta$  and do not conserve the energy flux. In this and subsequent papers, we will derive several classes of exact solutions to the cKP equation with different parameters  $\sigma^2 = \pm 1$  and discuss their relevance to physical phenomena.

Before we proceed further, it is necessary to mention two conserved quantities, which are of physical importance. Note that function  $U(r, \theta, \tau)$  must be periodic on the azimuthal variable  $\theta$  together with its derivatives with respect to  $\theta$ ; then, Eq. (1.2) can be integrated once over a period of  $\theta$ ; and then, it can be integrated once again over time  $t$  from minus to plus infinity under the assumption

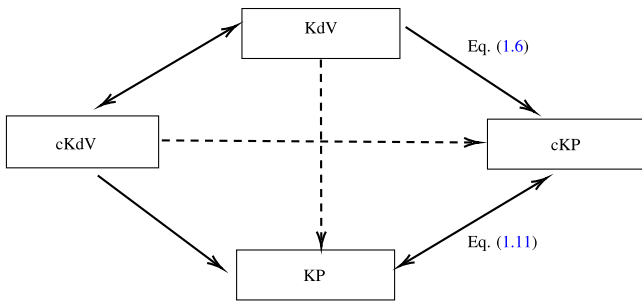


**FIG. 1.** The diagram that shows links between four relative equations.<sup>32</sup> One-way arrows stand for that all solutions of one-dimensional equations KdV and cKdV can be transformed into some particular solutions of two-dimensional equations KP and cKP, respectively, by means of the relevant transformation, but not vice versa. Two-way arrows stand for that there is one-to-one conformity between solutions of the corresponding equations. Dashed arrows show that all solutions of one-dimensional equations KdV and cKdV are, certainly, particular solutions of their two-dimensional counterparts, KP and cKP, respectively.

that function  $U(r, \theta, \tau)$  vanishes together with all its derivatives with respect to  $\tau$  when  $\tau \rightarrow \pm\infty$ . This gives a quantity  $I_1$  (see below), which can be interpreted as the “mass flux” of a pulse-type wave perturbation. Another quantity,  $I_2$ , that can be interpreted as the “energy flux,” can be derived if we preliminary multiply Eq. (1.2) by  $U$  and then integrate it over a period of  $\theta$  and over  $\tau$  as above. As a result of that, we obtain conserved quantities,

$$I_1 = \int_{-\infty}^{+\infty} \int_0^\Theta U(r, \theta, \tau) \sqrt{r} d\theta d\tau, \quad I_2 = \frac{1}{2} \int_{-\infty}^{+\infty} \int_0^\Theta U^2(r, \theta, \tau) r d\theta d\tau, \quad (1.4)$$

where  $\Theta = 2\pi\sqrt{6c(2/\beta c)^{1/3}}$  is a period of a function  $U$  [see Eq. (1.3)]. Physically reasonable solutions vanishing at plus and minus infinity on  $\tau$  must meet these requirements. For periodic in time solutions, the outer integrals must be evaluated over one period on  $\tau$ .

In the conclusion of this section, we will demonstrate that formal solutions of the cKP equation obtained from the KdV equation by the transformation of variables are physically irrelevant. As has been shown in Ref. 3, the cKP equation (1.2) can be reduced to the dimensionless “timelike KdV” (tKdV) equation,

$$\frac{\partial U}{\partial r} + 6U \frac{\partial U}{\partial \tau'} + \frac{\partial^3 U}{\partial \tau'^3} = 0, \quad (1.5)$$

with the help of the transformation

$$r = r, \quad \tau' = \tau - \frac{r\theta^2}{12\sigma^2}. \quad (1.6)$$

Using this transformation, one can formally obtain a wide family of “exact solutions” from the tKdV equation. Let us consider, in particular, a soliton solution to the tKdV equation (1.5),

$$U(\tau, r) = A \operatorname{sech}^2 \frac{1}{T} \left( \tau' - \frac{r}{V} \right), \quad T = \sqrt{\frac{2}{A}}, \quad V = \frac{1}{2A}. \quad (1.7)$$

Note that in this form, the soliton speed dependence on the amplitude looks unusual as it is inversely proportional to the amplitude  $A$  so that a soliton of a smaller amplitude moves faster than a soliton of a bigger amplitude within the framework of the tKdV equation (1.5). However, in physical variables, the dimensional soliton speed  $V_s$  is determined by the formula

$$V_s = \frac{c}{1 - (1/Vc)(\beta c/2)^{1/3}} = \frac{c}{1 - (2A/c)(\beta c/2)^{1/3}} \approx c \left[ 1 + 2 \frac{A}{c} (\beta c/2)^{1/3} \right].$$

The last approximate equality is valid for solitons of relatively small amplitudes  $A$ . Bearing in mind the link between the dimensional  $A_s$  and nondimensional  $A$  amplitudes as per Eq. (1.3), we obtain the usual relationship between the soliton amplitude and velocity:  $V_s \approx c(1 + \alpha A_s/3)$ .

Solution (1.7) under the transformation (1.6) provides the solution to the cKP equation (1.2),

$$U(\tau, r, \theta) = A \operatorname{sech}^2 \left\{ \sqrt{\frac{A}{2}} \left[ \tau - \left( 2A + \frac{\theta^2}{12\sigma^2} \right) r \right] \right\}. \quad (1.8)$$

If we fix the argument of this solution setting  $\tau - (2A + \theta^2/12\sigma^2)r = \tau_0$  then, we obtain the equation describing front propagation in the polar coordinates:

$$r(\tau, \theta) = \frac{\tau - \tau_0}{2A + \theta^2/12\sigma^2}. \quad (1.9)$$

As follows from this formula, the front size linearly increases with time. Figure 2 illustrates front shapes in the polar coordinates for  $-\pi \leq \theta \leq \pi$  for  $\sigma^2 = 1$  [frame (a)] and  $\sigma^2 = -1$  [frames (b) and (c)] at three different time moments. The solution is valid for  $r \gg 1$ ; therefore, the black circles in the center show the domains of the radius  $r = 10$  where the solution is invalid.

The main drawbacks of such solutions are (i) their fronts are either not smooth and contain cusps at  $\theta = \pm\pi$ , as shown in frames (a) and (b), or they go to infinity and are not periodic on  $\theta$ , as shown in frame (c); (ii) the soliton amplitude does not decrease with time and distance as should be expected for cylindrically diverging waves; therefore, mass and energy fluxes (1.4) do not conserve (this is the consequence of non-smoothness of the solution); and (iii) soliton fronts are shown for the specifically chosen angular interval  $-\pi \leq \theta \leq \pi$ , whereas beyond this interval, fronts become multi-valued. Thus, one can conclude that solutions that are formally derived through the transformation from the tKdV soliton, apparently, are not physically acceptable but can be considered curious mathematical constructions.

Similarly, one can see that the solutions to the cKP equation derived from the conventional KP equation<sup>9,17,33–36</sup> are also physically unacceptable. The link between solutions of the cKP equation (1.2) and the conventional KP equation in the form

$$\frac{\partial}{\partial x} \left( \frac{\partial U}{\partial t} + 6U \frac{\partial U}{\partial x} + \frac{\partial^3 U}{\partial x^3} \right) + 3\sigma^2 \frac{\partial^2 U}{\partial y^2} = 0, \quad (1.10)$$

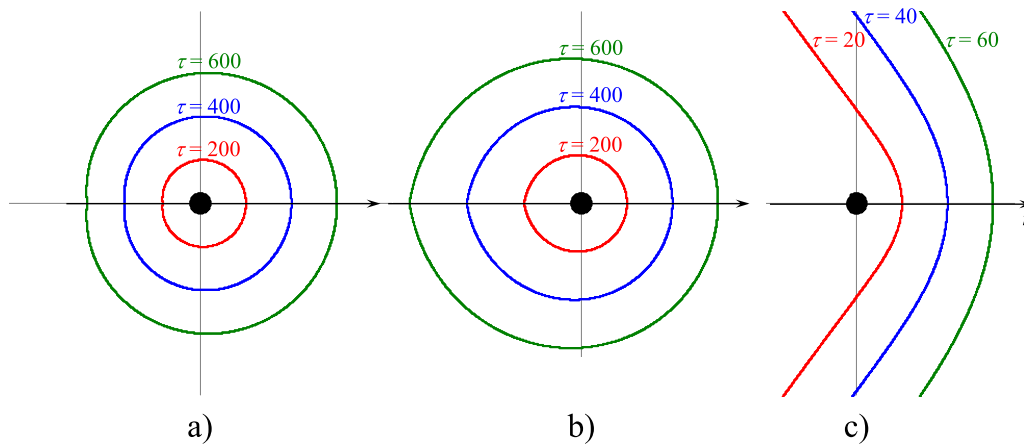


**FIG. 2.** Soliton fronts as per Eq. (1.8) at particular times. The parameters are  $\sigma^2 = 1, A = 2$  in frame (a);  $\sigma^2 = -1, A = 2$  in frame (b); and  $\sigma = -1, A = 0.2$  in frame (c). Black circles in the center show the domain where Eq. (1.2) is invalid.

where  $x$  and  $y$  are Cartesian coordinates, is given by the transformation<sup>36</sup>

$$U(x, y, t) \rightarrow U(r, \varphi, \tau), \quad x = \tau - \frac{r\theta^2}{12\sigma^2}, \quad y = r\theta, \quad t = r. \tag{1.11}$$

Here,  $U(x, y, t)$  is a solution of the KP equations (1.10), and  $U(r, \varphi, \tau)$  is the corresponding solution to the cKP equation (1.2). Such a transformation provides solutions, which are either non-smooth or discontinuous, or multivalued. In Secs. II and III and the next part of this study, we will present physically acceptable solutions constructed directly for the cKP or cKdV equations not using the transformation techniques.

## II. RING SOLITONS IN THE CKDV AND CKP EQUATIONS

As a first step, let us consider axis-symmetric solutions to the cKP equation (1.2) when the function  $U$  does not depend on  $\theta$ . In this case, Eq. (1.2) reduces to the cKdV equation, and its exact solutions were obtained in Refs. 40–42 (their asymptotic solutions were studied in Refs. 43 and 44). Solutions can be expressed through the Hirota transform<sup>45</sup> in terms of the auxiliary function  $\Gamma$ ,

$$U(r, \tau) = 2 \frac{\partial^2}{\partial \tau^2} \ln \Gamma. \tag{2.1}$$

The simplest “one-soliton solution” is

$$\Gamma = 1 + \frac{q}{(12r)^{1/3}} \left\{ z(r, \tau) W^2(z) - [W'(z)]^2 \right\}, \tag{2.2}$$

where  $q$  is an arbitrary parameter,  $W(z)$  is an Airy function either of the first kind or of the second kind, and  $z(r, \tau) = (\tau - \tau_0)/(12r)^{1/3}$ . The symbol prime stands for differentiation with respect to the argument of a function  $W$ . Note that in terms of the function  $\Gamma(r, \tau)$ , solution (2.2) is the typical self-similar solution on the constant pedestal. However, in the variable  $U(r, \tau)$ , the corresponding

solution is more complicated, and it is neither self-similar nor a traveling-wave solution,

$$U(r, \tau) = \frac{2}{(12r)^{2/3}} \frac{[(12r)^{1/3} + qF(z)] qF'(z) - q^2 [F'(z)]^2}{[(12r)^{1/3} + qF(z)]^2}, \tag{2.3}$$

where  $F(z) = z(r, \tau) W^2(z) - [W'(z)]^2$ . A genuine self-similar solution in terms of a function  $U(r, \tau)$  can be obtained from Eq. (2.3) if we set  $|q| \rightarrow \infty$ . Then, we obtain<sup>46</sup>

$$U(r, \tau) = \frac{2}{(12r)^{2/3}} \frac{FF'' - (F')^2}{F^2}. \tag{2.4}$$

Such a solution with the Airy function of the first kind,  $W(z) \equiv \text{Ai}(z)$ , was considered by Johnson<sup>3</sup> in application to a water-wave problem. The shapes of the self-similar solutions with the Airy functions of the first kind,  $\text{Ai}(z)$ , and the second kind,  $\text{Bi}(z)$ , are shown in Fig. 3. The solution shown in Fig. 3(b) is, obviously, singular at  $r = 0$ . [In this figure and all subsequent ones, we show  $U(t, r, \varphi) = \alpha u(t, r, \varphi)/6$ .]

In general, a self-similar solution to the cKdV equation can be derived directly from the cKdV equation if we seek a solution of Eq. (1.2) in the form  $U(r, \tau) = r^\alpha S(\xi)$ , where  $\xi = r^\beta \tau^\gamma$  (such an approach was used in Ref. 10 for the KdV equation). Substituting this form of the solution in Eq. (1.2), we obtain after simple manipulation that function  $S(\xi)$  must satisfy the ODE,

$$S''' + 6SS' - \frac{1}{3}\xi S' - \frac{1}{6}S = 0, \tag{2.5}$$

provided that  $\alpha = -2/3, \beta = -1/3, \gamma = 1$ . This agrees with the solution (2.4) if we set  $U(r, \xi) = 2S(\xi)/(12r)^{2/3}$ .

The order of the ODE (2.5) can be reduced by multiplication by  $S$  and integration with respect to  $\xi$  subject to zero boundary condition at plus and minus infinity; this gives<sup>6</sup>

$$SS'' - \frac{1}{2}(S')^2 + 2S^3 - \frac{1}{6}\xi S^2 = 0. \tag{2.6}$$

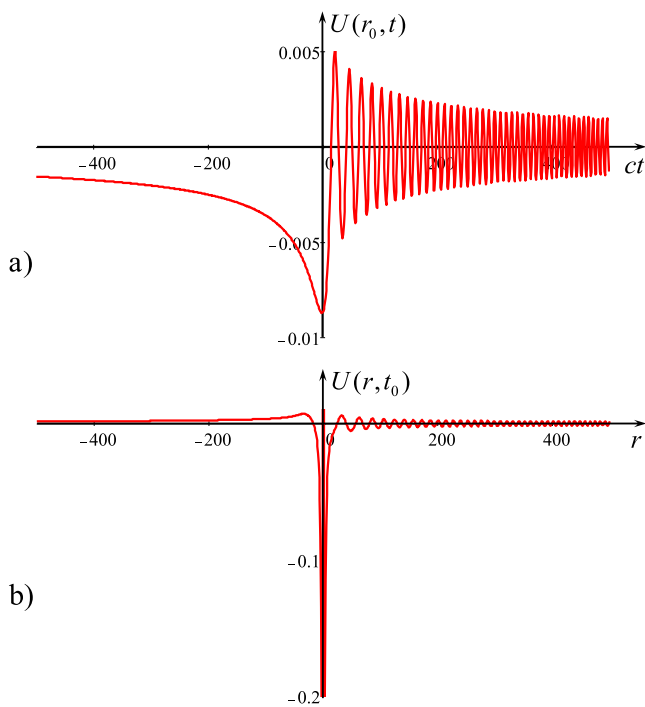


**FIG. 3.** Self-similar solutions to Eq. (1.1) as functions of the normalized time  $ct$  in terms of the Airy functions of the first kind  $Ai(z)$  [panel (a)] and second kind,  $Bi(z)$  [panel (b),  $r_0 = 306$ ]. In panel (a), the parameters are  $r_0 = 280$ ,  $c = 1$ ,  $\alpha = 1$ , and  $\beta = 2$  ( $\sigma = 1$ ). In panel (b), the parameters are  $r_0 = 306$ ,  $c = 1$ ,  $\alpha = -1$ , and  $\beta = -2$  ( $\sigma = i$ ).

Then, this equation can be reduced to the second Painlevé transcendent<sup>47,48</sup> through the substitution  $S = v^2$ ,

$$v'' - \frac{1}{12}\xi v + v^3 = 0 \tag{2.7}$$

(further details can be found in Ref. 6). A self-similar solution to the cKdV equation was also obtained differently in Ref. 63.

In what follows, we will focus on solitary-type solutions with circular fronts (ring solitons). The shape of a single ring soliton depends on the choice of the Airy function  $W$  in Eq. (2.2), as well as on the parameters  $q$  and  $\sigma$  in Eq. (1.2). Below, we present the analysis of solutions for both kinds of Airy functions.

### A. Ring solitons described by the Airy function of the first kind

Consider the first solution (2.3) with the Airy function of the first kind  $Ai(z)$  dubbed the Ai-soliton. To get a solution that resembles a classical KdV soliton, it is necessary to choose a very big on absolute value but negative parameter  $q$ . In the original variables, solution (2.3) depends on  $r$  and  $z(r, t)$ , where

$$z(r, t) = \sigma c \left( \frac{2}{|\beta|c} \right)^{1/3} \frac{r - ct}{(12r)^{1/3}}. \tag{2.8}$$

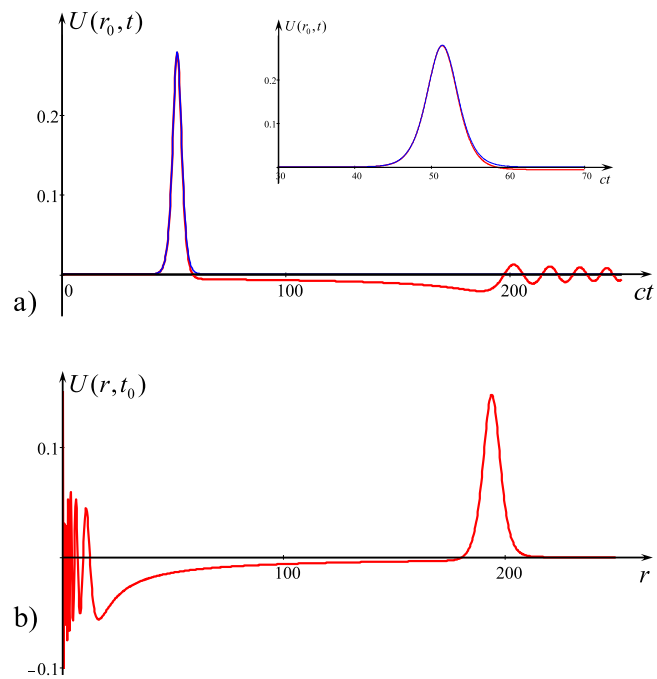


**FIG. 4.** The Ai-soliton with  $q = -10^{30}$  in the normalized variables. Panel (a) shows the dependence of  $U$  on the normalized time  $ct$  at the fixed distance  $r_0 = 75$  (red line). Panel (b) shows the dependence of  $U$  on distance  $r$  at the fixed time  $ct_0 = 125$ . Other parameters are  $c = 1$ ,  $\alpha = 1$ ,  $\beta = 2$ , and  $\sigma = 1$ . The blue line in panel (a) shows the shape of a plane KdV soliton of the same amplitude [solution (1.7) to Eq. (1.5)]. The insertion shows the magnified portion of the plot depicted in panel (a).

Figure 4 shows one of such solutions in the case of the “normal dispersion” when  $\beta > 0$  ( $\sigma = 1$ ) and  $q = -10^{30}$ . In panel (a), the solution is shown by the red line as a function of normalized time for a fixed distance  $r_0 = 75$ . In Fig. 4(b), the same solution is shown as a function of distance for the fixed normalized time  $ct_0 = 125$ . For the comparison, we show also by the blue line in panel (a) the shape of a plane KdV soliton of the same amplitude [solution (1.7) to Eq. (1.5)]. As one can see, the difference between these solutions is only in the tail part. The insertion in panel (a) shows the magnified portion of the plot depicted in panel (a). Note that if the nonlinear coefficient  $\alpha$  is negative, then the plots in Fig. 4 are mirror-symmetric with respect to the horizontal axes.

The Ai-soliton depicted in Fig. 4 represents an outgoing wave; i.e., it travels to the right along the  $r$  axis when time increases. In the vicinity of zero, the solution becomes oscillating with increasing frequency and amplitude. However, both the cKdV and cKP equations are inapplicable in the vicinity of  $r = 0$ ; therefore, this part of the solution is out of physical meaning and should be ignored.

In the case of the “abnormal dispersion” when  $\beta < 0$  ( $\sigma = i$ ) in Eq. (1.1), a solution based on the Airy function of the first kind,  $Ai(z)$ , looks qualitatively similar but in the reverse order in time and in space so that the oscillatory wavetrain arrives first and the pulse

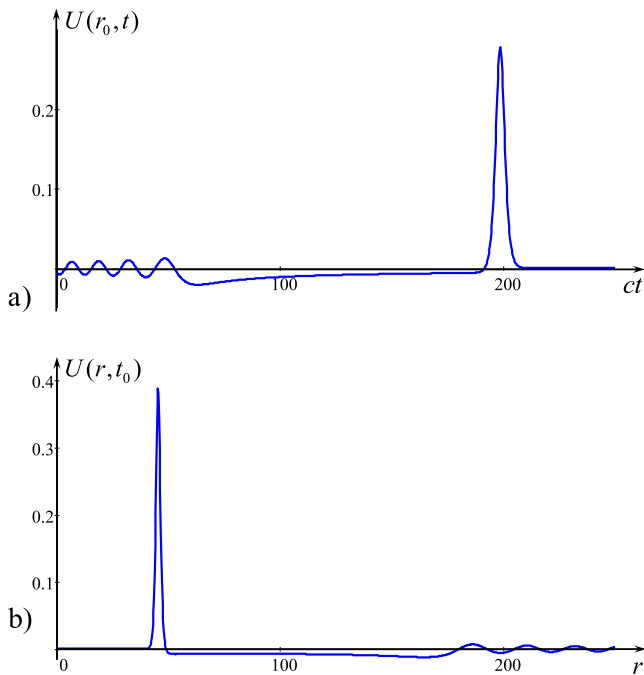


**FIG. 5.** The same as in Fig. 4 but with different parameters ( $\alpha = -1$ ,  $\beta = -2$ ,  $\sigma = i$ ). Panel (a): solution as a function of time  $ct = 100$  at a fixed distance  $r_0 = 75$ ; panel (b) – solution as a function of distance  $r$  at a fixed time  $t_0 = 50$ .

follows it. The polarity of the pulse is positive for the negative coefficient  $\alpha$ . An example is shown in Fig. 5. The solution describes a wave traveling to the right; i.e., it represents an outgoing perturbation.

In Fig. 6, we show solutions (2.3) based on the Ai-function with the different parameter  $q$ . When  $q \rightarrow -\infty$ , the solution becomes indeed similar to a KdV soliton in its leading part [see Fig. 6(a)]. The leading pulse is accompanied by a small-amplitude trailing wave. However, when the parameter  $q$  increases (decreases on the absolute value), the amplitude of the oscillatory tail becomes comparable with the amplitude of the leading pulse and even exceeds it [see, for instance, Fig. 6(d)]. For any positive parameter  $q > 0$ , the solution is singular.

**B. Ring solitons described by the Airy function of the second kind**

Consider now a solution based on the Airy function of the second kind  $Bi(z)$ . A solution with a solitary wave in the leading part (dubbed the Bi-soliton) now exists in the case of “abnormal dispersion” when  $\beta < 0$  ( $\sigma = i$ ). In the original variables, solution (2.3) depends on  $r$  and  $z$ , but now,

$$z(r, t) = c \left( \frac{2}{|\beta|c} \right)^{1/3} \frac{ct - r}{(12r)^{1/3}}. \tag{2.9}$$

A solitary-type solution can be obtained if we set a very small and positive parameter  $q \ll 1$ . Figure 7 shows one of such solutions with

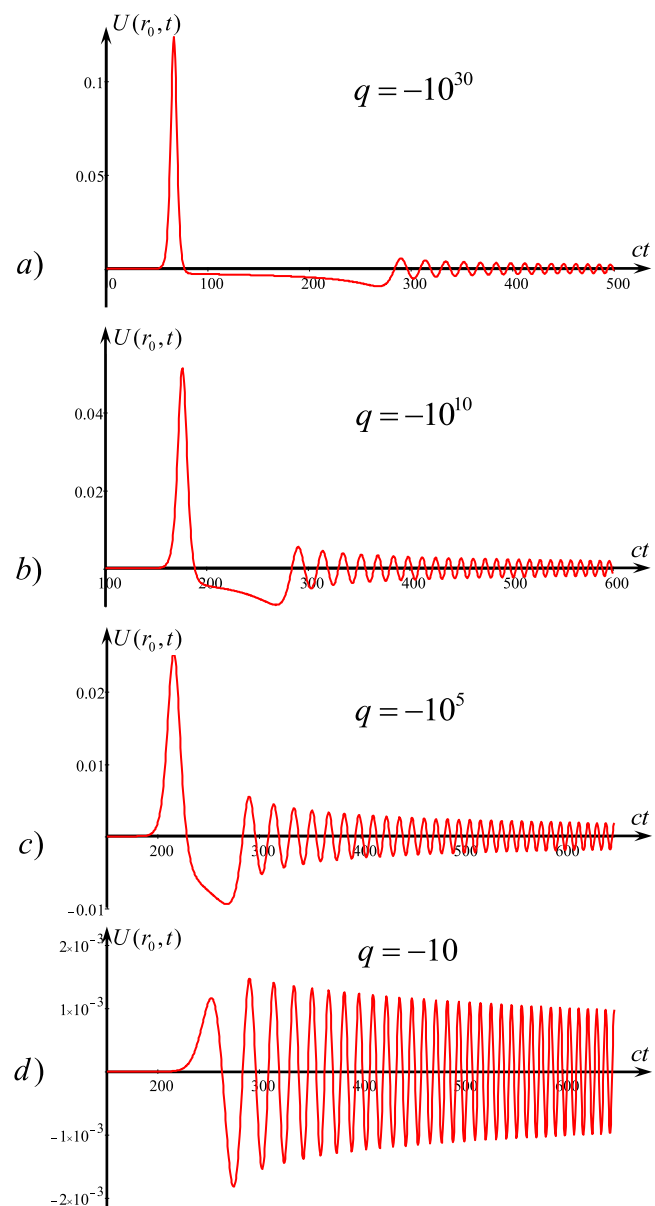


**FIG. 6.** Exact solutions to the cKdV equation (1.1) based on the Ai-function in the normalized variable  $U$  [see (1.3)] as functions of  $ct$  at a fixed distance  $r_0 = 250$ . (a)  $q = -10^{30}$ , (b)  $q = -10^{10}$ , (c)  $q = -10^5$ , and (d)  $q = -10$ . Other parameters were are  $c = 1$ ,  $\alpha = 1$ ,  $\beta = 2$ , and  $\sigma = 1$ . Note that the vertical and horizontal scales are different in different frames.

$q = 10^{-30}$  as a function of time for the fixed distance  $r_0 = 75$  [red line in panel (a)] and as a function of distance for the fixed time  $ct_0 = 125$  [panel (b)]. For the comparison, we show also in panel (a) a shape of a plane KdV soliton of the same amplitude (blue line). As one can see, the difference between the Bi-soliton and the KdV soliton is again only in the tail part, but the pulse tail now

25 January 2024 23:09:18

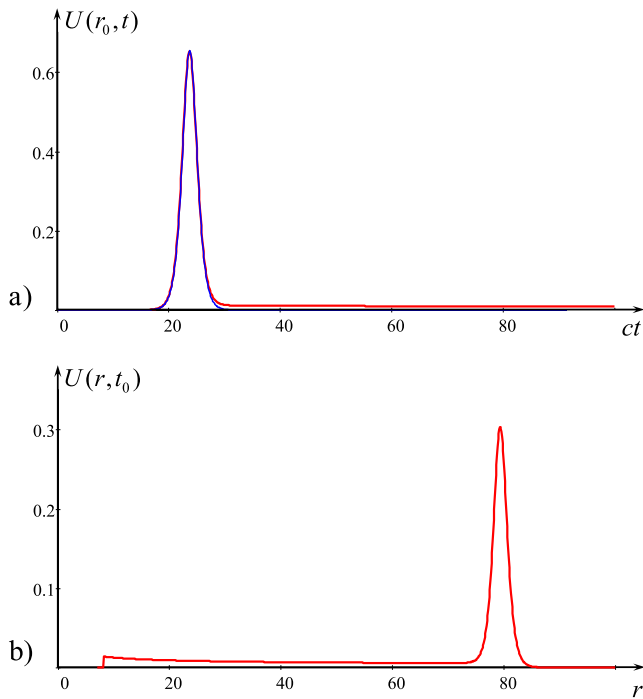


**FIG. 7.** The Bi-soliton with  $q = 10^{-30}$  in the normalized variables at the fixed distance  $r_0 = 75$  [red line in panel (a)] and as a function of distance  $r$  at the fixed time  $ct_0 = 225$  [panel (b)]. Other parameters are  $c = 1$ ,  $\alpha = -1$ , and  $\beta = -2$  ( $\sigma = i$ ). A meaningless part of the solution near  $r = 0$  was removed. The blue line in panel (a) shows the shape of a plane KdV soliton of the same amplitude.

decreases monotonically without oscillations. The solution describing the Bi-soliton becomes singular near the center where  $r = 0$ , but, as aforementioned, the cKdV and cKP equations are inapplicable in the vicinity of the center; therefore, this part of the solution is out of physical meaning; it was removed from Fig. 7(b). However, a solution based on the Bi Airy function has another singularity at a very big distance in front of the leading pulse. The position of the singularity quickly goes to infinity in terms of  $r$  (or to minus infinity in terms of  $t$ ) when  $q \rightarrow 0$ . Therefore, such a solution with extremely small  $q$  as shown, for example, in Fig. 7 could also be acceptable, in principle, for the interpretation of physical and numerical experiments given that both singularities, at  $r = 0$  and  $r \gg 1$ , are out of the physical meaning and can be ignored. For negative  $q$ , the solution has a singularity instead of a pulse at some finite distance. The Bi-soliton depicted in Fig. 7 represents an outgoing wave; i.e., it travels to the right along the  $r$  axis when time increases.

In Fig. 8, we show solutions (2.3) based on the Bi-function with the different parameter  $q$ . When  $q \rightarrow 0_+$ , the solution becomes indeed similar to a KdV soliton in its leading part [see Fig. 8(a)]. The leading pulse is accompanied by a small-amplitude smoothly decreasing tail of the same polarity as the pulse. However, when the parameter  $q$  increases, the amplitude of the tail becomes notable. For the relatively big  $q$ , an oscillatory train appears in front of the pulse

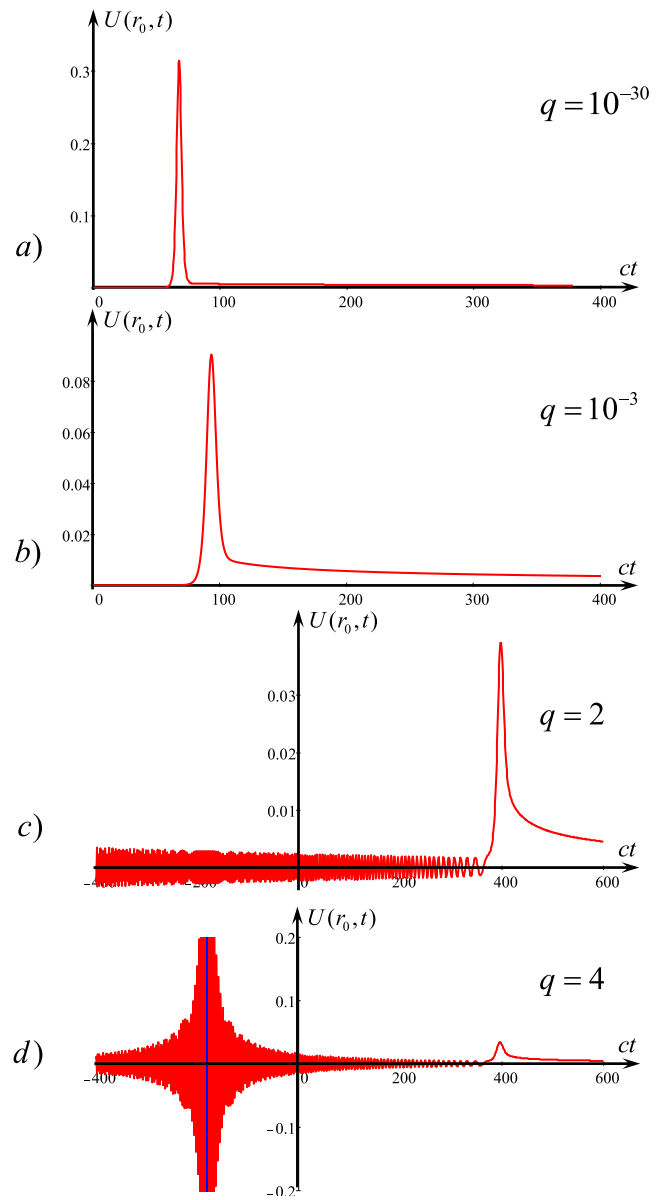


**FIG. 8.** Exact solutions to the cKdV equation (1.1) based on the Bi-function in the normalized variable  $U$  [see (1.3)] as functions of  $ct$  at a fixed distance  $r_0 = 75$ . (a)  $q = 10^{-30}$ , (b)  $q = 10^{-3}$ , (c)  $q = 2$ , and (d)  $q = 4$ . Other parameters are  $c = 1$ ,  $\alpha = -1$ ,  $\beta = -2$ , and  $\sigma = i$ . The vertical blue line in frame (d) shows a position of a singularity; on other frames, a position of a singularity is too far on the left. Note that the vertical and horizontal scales are different in different frames.

[see Figs. 8(c) and 8(d)]. The amplitude of oscillations increases at negative  $t$  and ends up at the point of singularity, which is not visible in Fig. 8(c) but quite visible in Fig. 8(d). For any negative parameter  $q < 0$ , the solution is singular.

In the case of the “normal dispersion” when  $\beta > 0$  ( $\sigma = 1$ ) in Eq. (1.1), a Bi-soliton looks qualitatively similar but in the reverse order in time so that its long “tail” arrives first, and the pulse follows it when the wave propagates to the right (outgoing circular wave). The polarity of the pulse is positive for the negative coefficient  $\alpha$  and vice versa.

The structure of solutions with the positive and negative  $\beta$  is quite understandable from the physical point of view. Indeed, in the normal dispersion case, the bigger the wavelength, the greater the wave speed; therefore, the “tail” having a much greater characteristic length than the pulse must propagate in front of it. In the case of abnormal dispersion, the situation is reversed. The bigger the wavelength, the smaller the wave speed; therefore, the long-wave “tail” must propagate behind the pulse. The same qualitative explanation is applicable to the structure of Ai-solitons.

### C. Comparison of analytical and numerical solutions for ring waves in the cKdV equation

To investigate the realizability of a solitary-type solution, we undertook direct numerical simulations of ring waves with initial perturbation in the form of the KdV soliton. For such a perturbation, an approximate solution can be constructed by the asymptotic method (see, e.g., Ref. 49 and references therein). In the leading order of the asymptotic theory, the solution is a KdV soliton with slowly varying parameters in space,

$$U(r, \tau) = A(r) \operatorname{sech}^2 \frac{\tau - \int dr/V(r)}{T(r)}. \quad (2.10)$$

The dependence of soliton amplitude on  $r$  can be found from the equation of energy flux conservation [see the quantity  $I_2$  in Eq. (1.4)]. Substituting there solution (2.10) and bearing in mind the relationship between  $T$  and  $A$ , we readily derive

$$A(r) = A_0 \left( \frac{r}{r_0} \right)^{-2/3}, \quad T(r) = T_0 \left( \frac{r}{r_0} \right)^{1/3}, \quad (2.11)$$

$$V(r) = \frac{1}{2A(r)} = \frac{1}{2A_0} \left( \frac{r}{r_0} \right)^{2/3}.$$

These dependences of parameter variations in nonlinear circular waves were obtained by means of approximate methods in several papers.<sup>50–55</sup> They are in perfect agreement with the exact solutions presented above for the Ai- and Bi-solitons,<sup>40–42</sup> as well as with the experimental and numerical data.<sup>22,54,60–63</sup> In Fig. 9, we show the result of the direct numerical modeling of the evolution of the initial KdV soliton with the amplitude  $A_0 = 0.3$  within the cKdV equation (1.1). The “initial condition” was actually set at the finite distance from the center at  $r_0 = 200$  as a function of time (it was rather a boundary condition).

A few important features of the result obtained can be noted.

- First, the shape of the leading pulse is indistinguishable from the shape of the KdV soliton of the same local amplitude and is well described by the asymptotic theory with the adiabatic variation of parameters as per Eq. (2.11).
- Second, in the course of pulse propagation, a long tail emerges behind it; its shape is shown in the insertion to Fig. 9 (see also

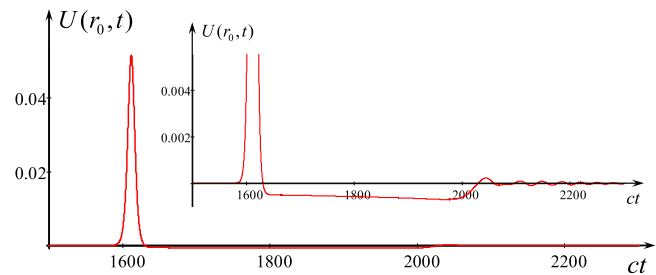
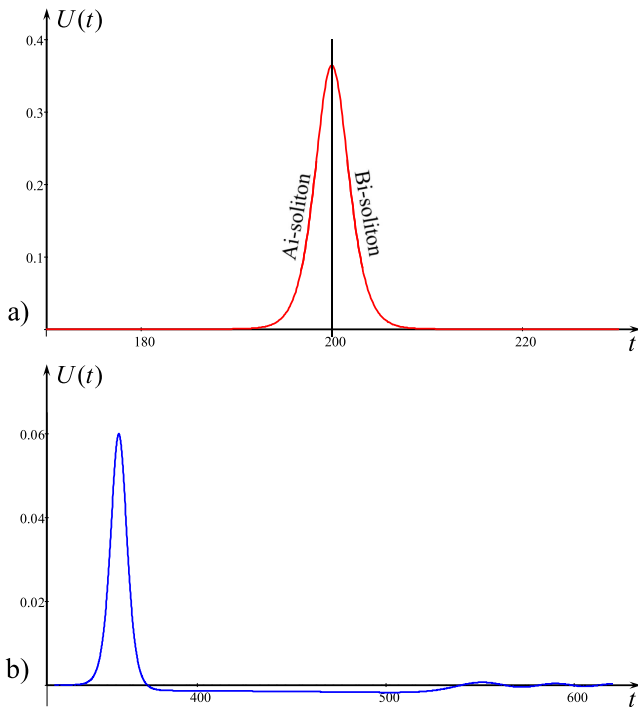


FIG. 9. The result of the numerical solution of the cKdV equation (1.1) with the “initial condition” in the form of the KdV soliton with the amplitude  $A_0 = 0.3$  at  $r_0 = 200$  as a function of time. Insertion shows a zoomed fragment of the solution demonstrating the tail structure behind the leading pulse.

Fig. 1 in Ref. 55 and Fig. 4 in Ref. 64). The tail shape can be described in the next order of the asymptotic theory; this has been done by Johnson<sup>64</sup> who derived the analytical expression for the tail both in the near-field zone (the negative polarity shelf) and the far-field zone (quasi-sinusoidal wavetrain). The shelf amplitude decays with the distance in the same manner as the leading pulse amplitude, i.e., as  $r^{-2/3}$  (Refs. 5 and 64). As one can see, the tail shape is very similar to the tail behind the Ai-soliton shown in Fig. 4(a).

- In the numerical study, we never observed the formation of a solitary-type solution with a shape similar to the shape of Bi-soliton with a long monotonically decaying tail as shown in Fig. 7. Apparently, only solutions similar to Ai-solitons can be formed in the course of the evolution of pulse-type circular initial perturbations. In relation to this, we note that Johnson<sup>64</sup> mentioned that the choice of the Bi-function in place of the Ai-function (and even a linear combination of Ai- and Bi-functions) does not lead to a proper solution of the cKdV equation due to the inevitable singularity in the Bi-function. Mathematically, this is true, but a singularity can be at such a big distance from the leading pulse that physically, it can be treated as existing at infinity.
- Solution (2.10) with adiabatically varying parameters (2.11) does not conserve the “mass flux” of a soliton  $I_s$ , whereas the total “mass flux” of the solution  $I_1$  (1.4) is surely conserved. The “mass flux” associated with only soliton according to the adiabatic solution (2.10) increases with the distance as  $I_{isol} \sim r^{1/6}$ . This means that in the course of pulse propagation, the negative polarity tail is generated in the form of a shelf that carries a negative “mass flux”  $I_{sh} \sim -r^{1/6}$ .<sup>5,64</sup> The shelf amplitude decreases  $r^{-2/3}$ , and its width increases as  $r^{5/6}$ . However, the analysis of mass conservation within the primitive set of hydrodynamic equations shows that the total mass and, therefore, a genuine mass flux must be equal to zero.<sup>5,21,53,64</sup> This is not the case for the cKdV model in which the total “mass flux” is constant but not necessarily zero. Nevertheless, for the exact solution of the cKdV equation based on the Ai-function, the “mass flux” is identically zero,<sup>64</sup> whereas for the solution based on the Bi-function, the “mass flux” is undetermined given that the Bi-soliton formally has a singularity far from its head.





**FIG. 10.** (a) Time dependence of the combined Ai–Bi-soliton at  $r_0 = 408$ . (b) Time dependence of the combined Ai–Bi-soliton at  $r = 724$ . Numerical data were obtained for the following parameters:  $\alpha = 1$ ,  $\beta = 2$ ,  $c = 1$ , and  $A_0 = 0.3642$ .

For the sake of curiosity, we considered also the evolution of a combined Ai–Bi soliton. To this end, we prepared for the numerical study a pulse-type initial condition the left part of which was an Ai-soliton with the parameter  $q_1 = -10^{30}$  up to the maximal value shown in Fig. 4(a), and the right part was a Bi-soliton with the parameter  $q_2 = 0.503 \times 10^{-12}$  commencing from the maximum and then exponentially decaying. With such parameters  $q$ , both maximum values were the same; the initial condition is shown in Fig. 10(a). Thus, the initial condition consisted of two exact solutions smoothly matched at the maximum. The artificially generated pulse profile exactly coincided with the profile of a KdV soliton with the same amplitude.

However, a numerical solution of the cKdV equation with such an initial condition was different from the solution of a KdV soliton. Initially, the pulse decay was very weak, and only asymptotically, at a big distance, its decay was similar to the decay of a KdV soliton or Ai- and Bi-solitons,  $A(r) \sim r^{-2/3}$ —see Fig. 11. At this asymptotic stage, the solution was qualitatively similar to the Ai-soliton. A long negative polarity tail was formed behind the leading pulse followed by small-amplitude oscillations in the far zone as shown in Fig. 10(b) (cf. Figs. 4 and 9).

Moreover, when the combined initial pulse was multiplied by a factor of 3, it disintegrates onto two pulses in the course of propagation. Each of these pulses further evolved into KdV-type (or Ai-type)

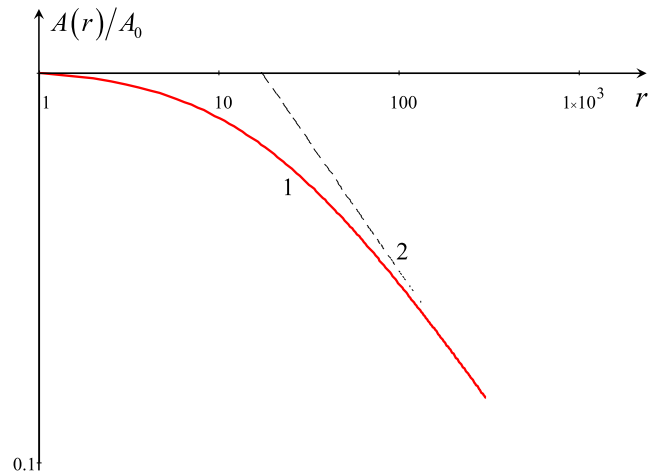


**FIG. 11.** The dependence of the normalized amplitude of the combined Ai–Bi soliton on the distance (line 1). Line 2 shows the asymptotic dependence  $A(r) \sim r^{-2/3}$ . Numerical data were obtained for the following parameters:  $\alpha = 1$ ,  $\beta = 2$ ,  $c = 1$ ,  $A_0 = 0.3642$ , and  $r_0 = 408$ .

solitons followed by negative polarity tails with oscillations in the far zone.

#### D. Interactions of cylindrical solitons in the cKdV equation

The Ai- and Bi-solitons can be considered counterparts of plane KdV solitons in the cylindrical geometry. As has been mentioned above, the cKdV equation is completely integrable; it possesses N-soliton solutions and an infinite number of conserved quantities; the first two of them are presented in Eq. (1.4), and others can be found, for example, in Ref. 42. Here, we will illustrate interactions of Ai- and Bi-solitons on the basis of two-soliton solutions derived by Nakamura and Chen.<sup>42</sup>

The “two-soliton solution” in terms of the function  $\Gamma(r, \tau)$  [see Eq. (2.2)] can be presented in the form<sup>42</sup>

$$\Gamma(r, \tau) = 1 + \varepsilon(a_{11} + a_{22}) + \varepsilon^2 \begin{vmatrix} a_{11} & a_{12} \\ a_{21} & a_{22} \end{vmatrix} = \begin{vmatrix} 1 + \varepsilon a_{11} & \varepsilon a_{12} \\ \varepsilon a_{21} & 1 + \varepsilon a_{22} \end{vmatrix}, \quad (2.12)$$

where the quantities  $a_{ij}$  are defined by the following expressions:

$$a_{ij} = \frac{\rho_i \rho_j}{(12r)^{1/3}} \frac{w_i(z_i) w'_j(z_j) - w'_i(z) w_j(z_j)}{z_i - z_j}, \quad i \neq j, \quad (2.13)$$

$$a_{ii} = \frac{\rho_i^2}{(12r)^{1/3}} \left\{ (z_i) w_i^2(z_i) - [w'_i(z_i)]^2 \right\}, \quad i = j, \quad (2.14)$$

where  $z_i = (\tau - \tau_i)/(12r)^{1/3}$ ,  $i, j = 1, 2$ , and  $w_i(z)$  are either Airy functions of the first kind  $\text{Ai}(z)$  or Airy functions of the second kind  $\text{Bi}(z)$ . The solution with the Bi-functions has been considered in Ref. 49 where they were treated (apparently, mistakenly) as

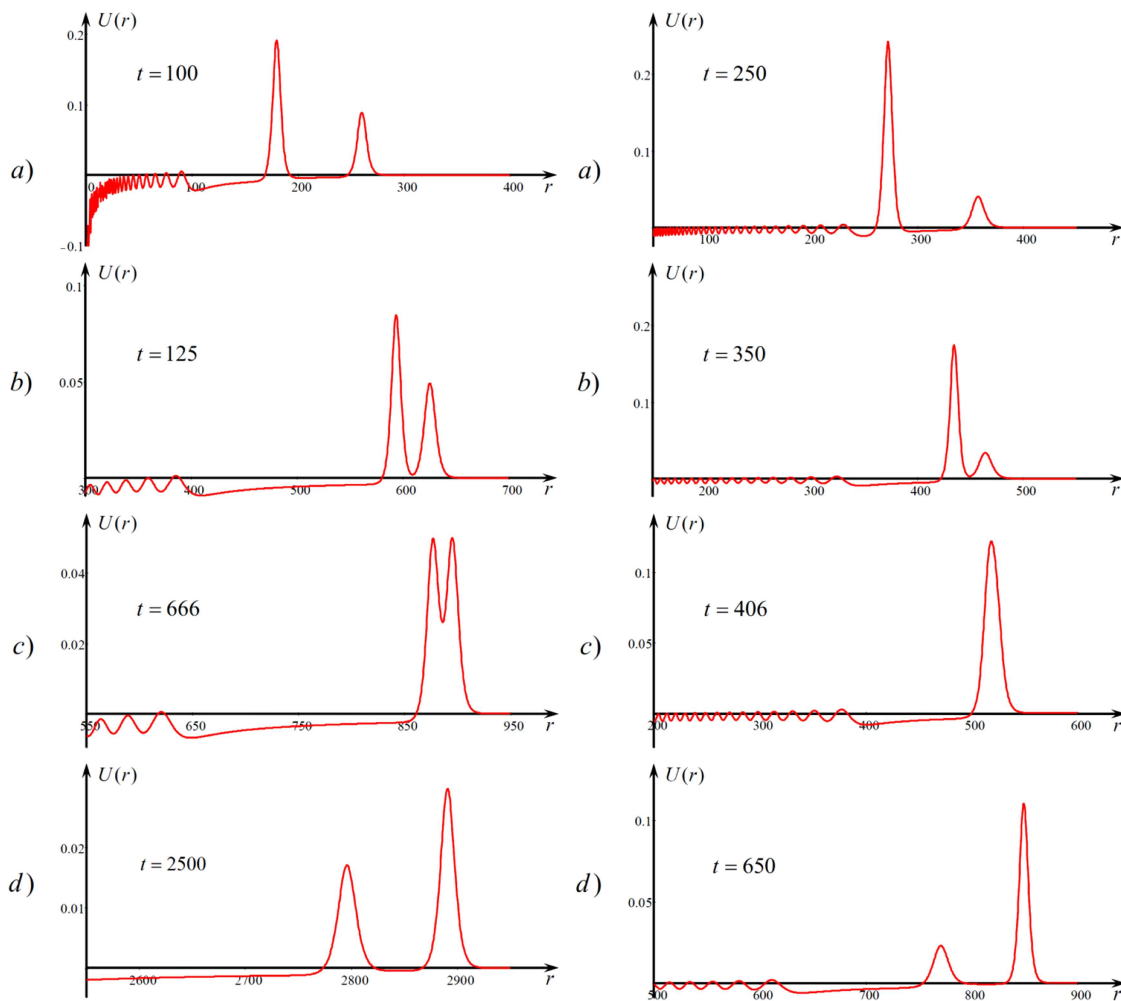


**FIG. 12.** Left column: Exchange type of soliton interaction with the following parameters:  $\varepsilon = 1$ ,  $\rho_1 = -10^{10}$ ,  $\rho_2 = -10^{20}$ ,  $\tau_1 = 24$ , and  $\tau_2 = -120$ . (a)  $t = 100$ , (b)  $t = 125$ , (c)  $t = 666$ , and (d)  $t = 2500$ . Right column: Overtaking type of soliton interaction with the following parameters:  $\varepsilon = 1$ ,  $\rho_1 = -10^5$ ,  $\rho_2 = -10^{40}$ ,  $\tau_1 = 24$ , and  $\tau_2 = -360$ . (a)  $t = 250$ , (b)  $t = 350$ , (c)  $t = 406$ , and (d)  $t = 650$ . Note that the vertical and horizontal scales are different in different frames.

the most relevant to the interpretation of physical and numerical experiments. Now, we consider that, namely, solutions based on the Ai-functions play such a role.

Similar to the classic KdV case, the character of the interaction of two Ai-solitons depends on their amplitudes. In the left column of Fig. 12, we illustrate the exchange type of soliton interaction when they do not completely overlap so that there is energy transformation from one of them into another one and in the right column—the overtaking type of interaction when they completely overlap at a certain time moment. Such interactions are well-known for the KdV<sup>65</sup> and some other equations. We did not study the details of a two-soliton interaction in the cylindrical case; this can be done elsewhere. Note that in the plane KdV case, there are two critical values of the soliton amplitude ratio. If the amplitude ratio  $A_1/A_2 < (3 + \sqrt{5})/2 \approx 2.62$ , the exchange-type interaction occurs, whereas, in the case of  $A_1/A_2 > 3$ , the overtaking-type interaction

occurs. A more complicated interaction occurs in the intermediate case,  $(3 + \sqrt{5})/2 < A_1/A_2 < 3$ . The details can be found in Ref. 65.

The N-soliton solution was also found by Nakamura and Chen.<sup>42</sup> The initial pulse fission onto a number of Ai-solitons can occur in the cylindrical case like in the plane case; some examples are presented in Ref. 49.

### III. STABILITY OF RING WAVES AND LUMP CREATION

Ring solitons considered in Sec. II can be subject to instability with respect to angular perturbation. By analogy with the plane case, intuitively, it is clear that instability can occur in media with positive dispersion when the coefficient  $\beta$  in Eq. (1.1) is negative.<sup>18,66–69</sup> However, the rigorous study of azimuthal instability of Ai-solitons has not been performed thus far. Krechetnikov<sup>6</sup> investigated the stability of a self-similar solution with respect to azimuthal perturbations

25 January 2024 23:09:18

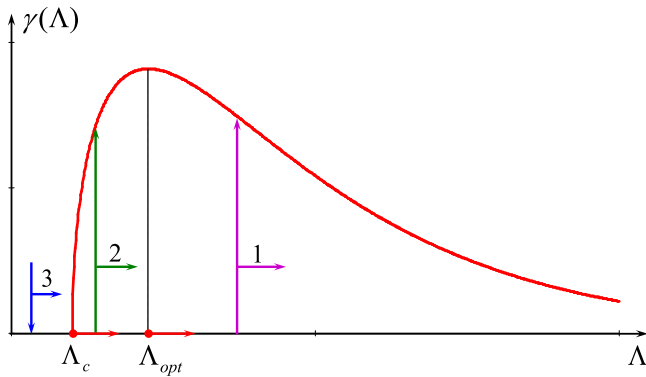


**FIG. 13.** Schematic illustration of different scenarios of modulation instability of a ring soliton with respect to azimuthal perturbations. Numbers 1, 2, and 3 correspond to the scenario number described in the text.

and confirmed that stability indeed occurs in media with negative dispersion,  $\beta > 0$ , but in media with positive dispersion,  $\beta < 0$ , the instability can occur under certain conditions and manifests in a complicated way. Here, we present first qualitative thoughts on the azimuthal instability of solitons, and then, we will demonstrate the development of instability through numerical modeling and some analytical solutions. To this end, we recall the condition of transverse instability of plane KdV solitons within the framework of the standard KP1 equation (1.10).

### A. Qualitative description of azimuthal instability of cylindrical solitons in the cKP1 equation

According to well-known results,<sup>66,67,69</sup> the instability of a KdV soliton of the amplitude  $A$  modulated in the lateral direction,  $U = A \operatorname{sech}^2[(x - 2At)\sqrt{A/2}]$ , occurs if the wavelength of a sinusoidal perturbation of a soliton front along the perpendicular  $y$ -axis is big enough, i.e.,  $\Lambda > \Lambda_c \equiv 4\pi/(A\sqrt{3})$ . However, in the cylindrical case, a wavelength of an azimuthal perturbation is restricted by the circular front circumference. Assuming that a ring outgoing soliton is perturbed by a small-amplitude sinusoidal wave of an  $n$ th mode, we obtain that in the course of propagation, the wavelength of the perturbation increases as  $\Lambda(t) = 2\pi r(t)/n$ . In the meantime, the critical wavelength also increases with time because the soliton amplitude decreases with  $r(t)$  as  $A \sim r^{-2/3}$  [see Eq. (2.11)]; therefore,

$$\Lambda_c = \frac{4\pi}{A(r)\sqrt{3}} = \frac{4\pi\sqrt{3}}{3A(r_0)} \left(\frac{r(t)}{r_0}\right)^{2/3}. \quad (3.1)$$

Thus, instability can occur when

$$r(t) > \frac{1}{r_0^2} \left(\frac{2n\sqrt{3}}{3A_0}\right)^3. \quad (3.2)$$

If at the beginning  $r_0 > 2n\sqrt{3}/(3A_0)$ , then the instability immediately starts to develop but, perhaps, not at the maximal rate. The maximum growth rate of instability  $\gamma_{max}$  occurs for the perturbation

of the optimal wavelength  $\Lambda_{opt}$ , where<sup>66-69</sup>

$$\begin{aligned} \gamma_{max} &= \frac{2\sqrt{6}A^{3/2}}{9} = \frac{2\sqrt{6}r_0A_0^{3/2}}{9r}, \\ \Lambda_{opt}(t) &= \frac{2\pi\sqrt{3}}{A(t)} = \frac{2\pi\sqrt{3}}{A_0} \left(\frac{r}{r_0}\right)^{2/3}. \end{aligned} \quad (3.3)$$

Therefore, we can describe qualitatively possible scenarios of the development of modulation instability of circular solitons in media with positive dispersion.

1. If the wavelength of azimuthal modulation of a soliton front is greater than the optimal value  $\Lambda_{opt}$ , then the modulation increases but with a gradually decreasing growth rate because the wavelength of azimuthal modulation on a soliton front permanently increases due to the cylindrical divergence.
2. If the wavelength of azimuthal modulation is slightly greater than the critical value  $\Lambda_c$ , then a growth rate of instability increases, attains its maximal value  $\gamma_{max}$ , and then slowly decreases up to zero.
3. If the wavelength of azimuthal modulation is less than the critical value  $\Lambda_c$ , then the modulation decreases first, but then, it starts to grow when the wavelength  $\Lambda$  exceeds  $\Lambda_c$ . After that, the scenario of item 2 is realized.

This scenario is schematically shown in Fig. 13 where the red line shows a qualitative dependence of the modulation growth as a function of the wavelength of azimuthal perturbation. Points  $\Lambda_c$  and  $\Lambda_{opt}$  move to the right as the soliton ring radius  $r$  increases,  $\Lambda_c \sim \Lambda_{opt} \sim r^{2/3}$ . However, a wavelength  $\Lambda$  of any perturbation increases faster with the radius,  $\Lambda \sim r$ . Therefore, the wavelength of a perturbation overtakes the  $\Lambda_{opt}$  so that its growth rate gradually decreases especially since the maximum of the growth-rate curve also decreases  $\gamma_{max} \sim 1/r$  as per Eq. (3.3). Even if the wavelength of an azimuthal perturbation is less than the critical one,  $\Lambda_c$  (see line 3 in Fig. 13), there is still a chance to overtake the critical point  $\Lambda_c$  before the perturbation completely disappears. Then, the perturbation will start growing.

Thus, according to this analysis, the outgoing ring solitons are stable if  $\beta > 0$ . This pertains both to Ai- and Bi-solitons, the examples of which are shown in Figs. 4(b) and 7(b), respectively. In the case of  $\beta < 0$ , ring solitons are unstable with respect to azimuthal perturbations; one such unstable solitons is shown in Fig. 5(b). Below, we illustrate the aforementioned scenarios of instability by means of numerical modeling.

### B. Numerical modeling of azimuthal instability of cylindrical solitons in the cKP1 equation

The qualitative thoughts presented in Sec. III A agree well with the results of direct numerical modeling of azimuthal instability of ring Ai-solitons in the cKP1 equation (1.1) with  $\beta < 0$ . The initial ring Ai-soliton with the radius  $r_0 = 30$  and amplitude  $A_0 = 0.5129$  was slightly modulated on amplitude by a sinusoidal perturbation of mode 2 (the mode number is the number of wavelengths in the azimuthal direction) and the relative amplitude of modulation of 5% as shown in Fig. 14(a).

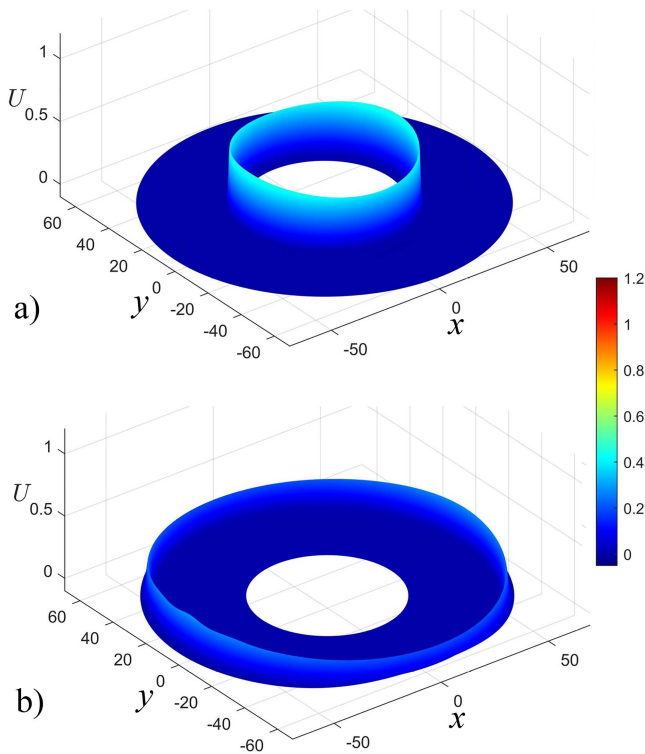


**FIG. 14.** Development of the modulation instability from the ring Ai-soliton with a small sinusoidal perturbation of soliton amplitude of mode 2. Frame (a)  $t = 140$  and frame (b)  $t = 240$ . The central part in each frame where the cKP equation (1.2) is invalid has been deleted. The plot was generated with the following parameters:  $c = 1$ ,  $\alpha = -1$ ,  $\beta = -2$ , and  $\sigma = i$ .

With this perturbation,  $\Lambda_c = 14.15$  according to Eq. (3.1) and  $\Lambda_{opt} = 21.22$  according to Eq. (3.3), whereas the wavelength of the perturbation is half of the circumference for the mode 2,  $\Lambda = \pi r_0 = 94.2 > \Lambda_c$ . In the process of evolution, the modulation increased, as was expected, and lump-type patterns commenced formation [see Fig. 14(b)]. However, because the wavelength of the modulation  $\Lambda$  is more than four times greater than the optimal, the growth rate of the perturbation is too small and becomes smaller and smaller when the radius of the ring wave increases. Therefore, in our numerical modeling due to restricted computer resources, we could see only the initial stage of development of very weak modulation instability.

The development of the modulation instability becomes more favorable for mode 4. In this case with the same initial amplitude, radius of the ring soliton, and 5% modulation, we have the wavelength of the perturbation of a quarter of the circumference,  $\Lambda = \pi r_0/2 = 47.1$ , which is only about two times greater than  $\Lambda_{opt} = 21.22$ . Now, the growth rate is sufficient for the formation of four lumps for a relatively short time as shown in Fig. 15. Such instability was observed for any type of initial soliton with a circular front.

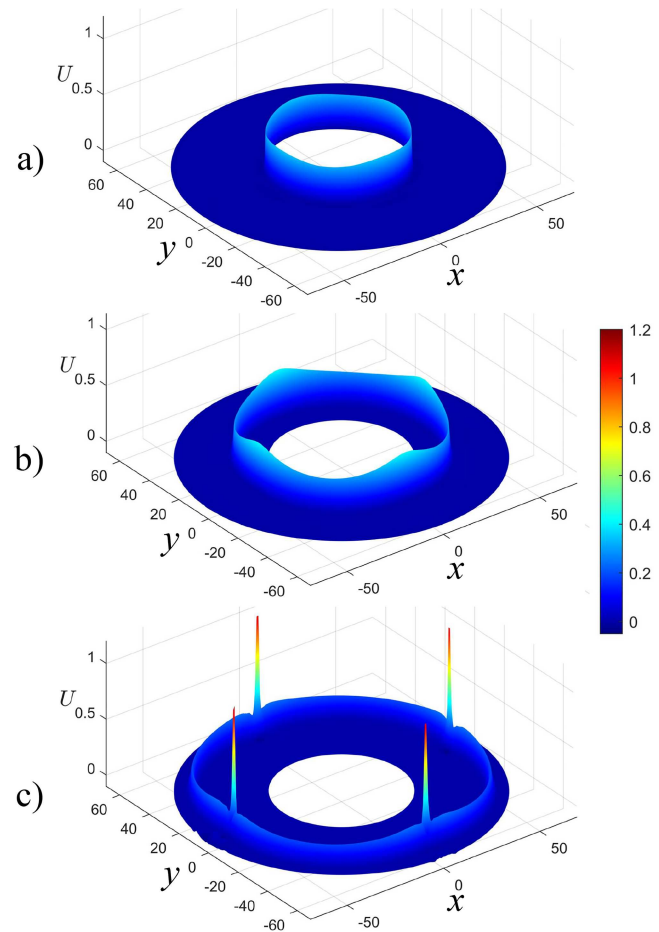


**FIG. 15.** Development of the modulation instability from the ring Ai-soliton with a small sinusoidal perturbation of soliton amplitude of mode 4. Frame (a)  $t = 120$ , frame (b)  $t = 170$ , and frame (c)  $t = 200$ . The central part in each frame where the cKP equation (1.2) is invalid has been deleted. The plot was generated with the following parameters:  $c = 1$ ,  $\alpha = -1$ ,  $\beta = -2$ , and  $\sigma = i$ .

In general, one can say that in the process of disintegration of an outgoing ring soliton, we observe the creation of lump chains with a different number of lumps on a circle front. The distance between lumps increases in the course of propagation, which makes such lump chains unstable with respect to azimuthal perturbation and creation of new chains and so on; a similar phenomenon is known for the quasi-plane case within the framework of the KP1 equation.<sup>70</sup> In the next paper, we will study analytically the interactions of circular solitons with lump chains as well as the normal and anomalous interactions of lump chains with each other.

#### IV. DISCUSSION AND CONCLUSION

In this paper, we presented a revised study of ring solitary waves described by the cylindrical Korteweg–de Vries equation. It was shown that the cKdV equation has two types of exact solutions that

can be expressed through the Airy functions of the first kind,  $Ai(z)$ , and the second kind,  $Bi(z)$ . Both these solutions look like KdV solitons and possess soliton properties (they can evolutionary emerge from initial pulses of specific shapes, re-emerge after interactions with each other, and others). Despite these solutions having singularities at  $r = 0$ , their leading parts that are far from the center can be relevant for the comparison with experimental and numerical data (note that the cKdV equation per se is valid only at a big distance from the center). However, a soliton solution described by the  $Bi(z)$ -function has an additional singularity far from the pulse maximum. Such a singularity can be very far, practically, at infinity if the soliton is well-pronounced. Meanwhile, our numerical study shows that in the process of evolution of an arbitrary pulse-type perturbation, the formation of a solution that resembles the  $Ai$ -soliton occurs. Such a formation was observed for several different pulses, but we never observed a formation of the  $Bi$ -type solitons.

Ring solutions studied in the paper can be subject to lateral modulation instability with respect to the azimuthal perturbations. Such instability can occur in media with positive dispersion. We presented a qualitative description of the instability and estimated parameters of the growth rate and range of instability. Our numerical modeling within the cKP equation demonstrates an agreement with the qualitative estimates. The development of modulation instability leads to the formation of lumps; more precisely, lump chains containing several lumps on a circular front. In the second part of this study, we will focus on lump dynamics, normal and anomalous interactions of lump chains, and other issues related to lumps and circular solitons.

## ACKNOWLEDGMENTS

Wencheng Hu acknowledges the funding provided by the China Scholarship Council (Grant No. 202002425001). Qi Guo and Zhao Zhang acknowledge the financial support provided by the Natural Science Foundation of Guangdong Province of China (Grant No. 2021A1515012214) and the Science and Technology Program of Guangzhou (Grant No. 2019050001). Yury Stepanyants acknowledges the funding of this study provided by the RF Council on Grants for the state support of Leading Scientific Schools of the Russian Federation (Grant No. NSH-70.2022.1z.5).

## AUTHOR DECLARATIONS

### Conflict of Interest

The authors have no conflicts to disclose.

## Author Contributions

**Wencheng Hu:** Formal analysis (equal); Investigation (equal); Software (equal); Validation (equal); Visualization (equal). **Zhao Zhang:** Formal analysis (equal); Investigation (equal); Validation (equal); Visualization (equal); Writing – original draft (equal). **Qi Guo:** Project administration (equal); Supervision (equal); Validation (equal). **Yury Stepanyants:** Conceptualization (equal); Formal analysis (equal); Investigation (equal); Methodology (equal); Project administration (equal); Supervision (equal); Validation (equal); Writing – original draft (equal); Writing – review & editing (equal).

## DATA AVAILABILITY

The data that support the findings of this study are available from the corresponding author upon reasonable request.

## APPENDIX: DERIVATION OF THE CKP EQUATION

Here, we present the derivation of the cylindrical KP equation from the model two-dimensional Boussinesq equation,

$$\frac{\partial^2 u}{\partial t^2} - c^2 \Delta (u + \alpha u^2) - \beta \Delta^2 u = 0, \quad (\text{A1})$$

where  $u$  is the wave perturbation,  $c$  is the speed of long linear waves,  $\alpha$  and  $\beta$  are the coefficients of nonlinearity and dispersion, respectively, and  $\Delta$  is the two-dimensional Laplace operator in the polar coordinates.

Let us re-write this equation in the extended form,

$$\frac{\partial^2 u}{\partial r^2} + \frac{1}{r} \frac{\partial u}{\partial r} + \frac{1}{r^2} \frac{\partial^2 u}{\partial \varphi^2} - \frac{1}{c^2} \frac{\partial^2 u}{\partial t^2} = -\alpha \left( \frac{\partial^2 u^2}{\partial r^2} + \frac{1}{r} \frac{\partial u^2}{\partial r} + \frac{1}{r^2} \frac{\partial^2 u^2}{\partial \varphi^2} \right) - \frac{\beta}{c^2} \Delta^2 u = 0. \quad (\text{A2})$$

We will consider a wave process on a big distance from the geometric center of the coordinate origin, assuming that  $r \gg \Lambda$ , where  $\Lambda$  is the characteristic width (wavelength) of a wave. We also assume that the effects of nonlinearity and dispersion are small. Formally, we assume that  $|\alpha| \ll 1$  and  $|\beta| \ll 1$ . Then, we remove to the right-hand side all higher-order terms leaving on the left-hand side the zero-order terms,

$$\frac{\partial^2 u}{\partial r^2} - \frac{1}{c^2} \frac{\partial^2 u}{\partial t^2} \approx -\frac{1}{r} \frac{\partial u}{\partial r} - \frac{1}{r^2} \frac{\partial^2 u}{\partial \varphi^2} - \alpha \frac{\partial^2 u^2}{\partial r^2} - \frac{\beta}{c^2} \frac{\partial^4 u}{\partial r^4}. \quad (\text{A3})$$

In this equation, higher-order terms were omitted. The first two terms on the right-hand side are small in comparison with the terms on the left-hand side because of the geometric factors  $1/r$  and  $1/r^2$ . The smallness of the nonlinear and dispersive terms on the right-hand side can be confirmed in a similar way. In particular, the estimation of the nonlinear term presumes that  $|\alpha|A^2/\Lambda^2 \ll A/\Lambda^2$ , where  $A$  is the characteristic wave amplitude. This leads to the condition  $|\alpha|A \ll 1$ . The similar estimation of the dispersive term gives  $|\beta|A/c^2\Lambda^4 \ll A/\Lambda^2$ , which leads to the condition  $\Lambda^2 \gg |\beta/c^2|$ . Therefore, the wave amplitude must be relatively small, and the wavelength must be large. The terms omitted in Eq. (A3) contain additional small parameters related to the geometrical factor.

The wave operator on the left-hand side can be factorized,

$$\left( \frac{\partial}{\partial r} - \frac{1}{c} \frac{\partial}{\partial t} \right) \left( \frac{\partial}{\partial r} + \frac{1}{c} \frac{\partial}{\partial t} \right) u = -\frac{1}{r} \frac{\partial u}{\partial r} - \frac{1}{r^2} \frac{\partial^2 u}{\partial \varphi^2} - \alpha \frac{\partial^2 u^2}{\partial r^2} - \frac{\beta}{c^2} \frac{\partial^4 u}{\partial r^4}. \quad (\text{A4})$$

In the zero approximation, when the higher-order terms on the right-hand side are neglected, Eq. (A4) describes, in general, two oppositely propagating waves obeying simple wave equations. One of them describes a diverging wave,  $\partial u/\partial r + (1/c)(\partial u/\partial t) = 0$ , and another one—a converging wave,  $\partial u/\partial r - (1/c)(\partial u/\partial t) = 0$ .

Let us consider a diverging wave; for such a wave, we have in the zero approximation the relationship between the derivatives  $\partial/\partial r = -(1/c)(\partial/\partial t)$ ; this relationship can be used in the higher-order terms. Replacing then spatial derivatives with the temporal derivatives on the right-hand side of Eq. (A4), we obtain the cKP equation in the form

$$\frac{\partial}{\partial t} \left( \frac{\partial u}{\partial r} + \frac{1}{c} \frac{\partial u}{\partial t} + \frac{u}{2r} - \frac{\alpha u}{c} \frac{\partial u}{\partial t} - \frac{\beta}{2c^5} \frac{\partial^3 u}{\partial t^3} \right) = \frac{c}{2r^2} \frac{\partial^2 u}{\partial \varphi^2}. \quad (\text{A5})$$

For long weakly nonlinear surface waves on water of the depth  $h$ , the coefficients are (see, for example, Refs. 16 and 71)

$$c = \sqrt{gh}, \quad \alpha = \frac{3}{2h}, \quad \beta = \frac{c^2 h^2}{3}, \quad (\text{A6})$$

$$c = \sqrt{g \frac{\delta \rho}{\rho} \frac{h_1 h_2}{h_1 + h_2}}, \quad \alpha = \frac{3}{2} \frac{h_1 - h_2}{h_1 h_2}, \quad \beta = \frac{c^2 h_1 h_2}{3}, \quad (\text{A7})$$

where  $h_1$ ,  $h_2$  are the thicknesses of the upper and lower layers, respectively,  $\rho$  is the average water density in both layers,  $\delta \rho$  is the difference between the densities of the layers, and  $g$  is the acceleration due to gravity.

Note also that the alternative heuristic cKdV-type equation was suggested in Ref. 57, but its merit is doubtful.

## REFERENCES

- <sup>1</sup> See <https://www.eumetsat.int/internal-waves-eastern-strait-gibraltar> for "Internal Waves in the Eastern Strait of Gibraltar."
- <sup>2</sup> L. G. Baehr, "The waves within the waves," *Oceanus* (December 2014); see <https://www.whoi.edu/oceanus/feature/the-waves-within-the-waves/>.
- <sup>3</sup> R. S. Johnson, "Water waves and Korteweg–de Vries equations," *J. Fluid Mech.* **97**(4), 701–719 (1980).
- <sup>4</sup> R. S. Johnson, "The classical problem of water waves: A reservoir of integrable and nearly-integrable equations," *J. Nonlinear Math. Phys.* **10**(Suppl. 1), 72–92 (2003).
- <sup>5</sup> R. H. J. Grimshaw, "Initial conditions for the cylindrical Korteweg–de Vries equation," *Stud. Appl. Math.* **143**(2), 176–191 (2019).
- <sup>6</sup> R. Krechetnikov, "Transverse instability of concentric soliton waves," [arXiv:2209.08628v1](https://arxiv.org/abs/2209.08628v1) (2022).
- <sup>7</sup> V. D. Lipovskii, "To the nonlinear theory of internal waves in a finite-depth fluid," *Izv. RAN Ser. Fiz. Atm. Okeana* **21**(8), 864–872 (1985) (in Russian).
- <sup>8</sup> W. Q. Peng, S. F. Tian, and T. T. Zhang, "Dynamics of the soliton waves, breather waves, and rogue waves to the cylindrical Kadomtsev–Petviashvili equation in pair-ion-electron plasma," *Phys. Fluids* **31**(10), 102107 (2019).
- <sup>9</sup> C. Klein, V. B. Matveev, and A. O. Smirnov, "Cylindrical Kadomtsev–Petviashvili equation: Old and new results," *Theor. Math. Phys.* **152**(2), 1132–1145 (2007).
- <sup>10</sup> V. I. Karpman, *Non-Linear Waves in Dispersive Media* (Pergamon Press, Oxford, New York, 1975).
- <sup>11</sup> M. Obregon and Y. Stepanyants, "Oblique magneto-acoustic solitons in a rotating plasma," *Phys. Lett. A* **249**, 315–323 (1998).
- <sup>12</sup> A. I. Potapov and I. N. Soldatov, "Quasi-plane beam of nonlinear longitudinal waves in a plate," *Sov. Phys. Acoust.* **30**(6), 486–488 (1984).
- <sup>13</sup> A. Alias, R. H. J. Grimshaw, and K. R. Khusnutdinova, "Coupled Ostrovsky equations for internal waves in a shear flow," *Phys. Fluids* **26**, 126603 (2014).
- <sup>14</sup> R. Grimshaw, "Effect of a background shear current on models for nonlinear long internal waves," *Fundam. Appl. Hydrophys.* **8**(3), 20–23 (2015).
- <sup>15</sup> A. Doak, G. Baardink, P. A. Milewski, and A. Souslov, "Nonlinear shallow-water waves with vertical odd viscosity," *SIAM J. Appl. Sci.* **83**, 938–965 (2023).
- <sup>16</sup> M. J. Ablowitz and H. Segur, *Solitons and the Inverse Scattering Transform* (SIAM, Philadelphia, PA, 1981), p. 425.

<sup>17</sup> N. Batoool, W. Masood, M. Siddiq, and R. Jahangir, "Exact solution of CKP equation and formation and interaction of two solitons in pair-ion-electron plasma," *Phys. Fluids* **23**, 082306 (2016).

<sup>18</sup> B. B. Kadomtsev and V. I. Petviashvili, "On the stability of solitary waves in weakly dispersing media," *Sov. Phys. Dokl.* **15**, 539–541 (1970).

<sup>19</sup> V. E. Zakharov, "Turbulence in integrable systems," *Stud. Appl. Math.* **122**, 219–234 (2009).

<sup>20</sup> S. V. Iordansky, "On the asymptotic of an axisymmetric divergent wave in a heavy fluid," *Dokl. Akad. Sci. USSR* **125**(6), 1211–1214 (1959).

<sup>21</sup> A. A. Lugovtsov and B. A. Lugovtsov, "Study of axisymmetric long waves in the Korteweg–de Vries approximation," in *Dynamics of Continuous Medium* (Institute of Hydrodynamics, Novosibirsk, 1969), Vol. 1, pp. 195–198 (in Russian).

<sup>22</sup> S. Maxon and J. Viecelli, "Cylindrical solitons," *Phys. Fluids* **17**(8), 1614–1616 (1974).

<sup>23</sup> R. S. Johnson, "Ring waves on the surface of shear flows: A linear and nonlinear theory," *J. Fluid Mech.* **215**, 145–160 (1990).

<sup>24</sup> K. R. Khusnutdinova, C. Klein, V. B. Matveev, and A. O. Smirnov, "On the integrable elliptic cylindrical Kadomtsev–Petviashvili equation," *Chaos* **23**, 013126 (2013).

<sup>25</sup> V. S. Dryuma, "Analytic solution of the two-dimensional Korteweg–de Vries (KdV) equation," *JETP Lett.* **19**(2), 387–388 (1974).

<sup>26</sup> V. S. Dryuma, "On the analytical solution of the axisymmetric KdV equation," *Izv. Akad. Nauk MSSR Ser. Fiz. Tekhnicheskikh Mat. Nauk* **3**, 87 (1976) (in Russian).

<sup>27</sup> V. S. Dryuma, "On the integration of the cylindrical Kadomtsev–Petviashvili equation by the method of the inverse problem of scattering theory," *Sov. Math. Dokl.* **27**, 6–8 (1983).

<sup>28</sup> R. Hirota, "Exact solutions to the equation describing 'cylindrical solitons,'" *Phys. Lett. A* **71**(5–6), 393–394 (1979).

<sup>29</sup> V. D. Lipovsky, V. B. Matveev, and A. O. Smirnov, "On the connection between the Kadomtsev–Petviashvili and Johnson equations," in *Problems of Quantum Field Theory and Statistical Physics* (Nauka, Leningrad, 1986), Vol. 6, pp. 70–75; *Zapisky Nauch. Seminar. LOMI* **150**, MR 88e:35171 (in Russian).

<sup>30</sup> A. Nakamura, "Solitons in high dimensions," *Prog. Theor. Phys. Suppl.* **94**, 195–209 (1988).

<sup>31</sup> S. P. Shen and M. C. Shen, "On a Korteweg–de Vries equation with variable coefficients in cylindrical coordinates," *Phys. Fluids* **29**(6), 1759–1760 (1986).

<sup>32</sup> Y. A. Stepanyants, "On the connections between solutions of one-dimensional and quasi-one-dimensional evolution equations," *Russ. Math. Surv.* **44**, 255–256 (1989).

<sup>33</sup> P. Gaillard, "Multiparametric families of solutions to the Johnson equation," *J. Phys.: Conf. Ser.* **1141**, 012102 (2018).

<sup>34</sup> P. Gaillard, "The Johnson equation, Fredholm and Wronskian representations of solutions, and the case of order three," *Adv. Math. Phys.* **2018**, 1642139.

<sup>35</sup> X. Z. Li, J. L. Zhang, and M. L. Wang, "Solitary wave solutions of KP equation, cylindrical KP equation and spherical KP equation," *Commun. Theor. Phys.* **67**, 207–211 (2017).

<sup>36</sup> V. D. Lipovskii, V. B. Matveev, and A. O. Smirnov, "Connection between the Kadomtsev–Petviashvili and Johnson equations," *J. Sov. Math.* **46**(1), 1609–1612 (1989).

<sup>37</sup> V. I. Golin'ko, V. S. Dryuma, and Yu. A. Stepanyants, "Nonlinear quasicylindrical waves: Exact solutions of the cylindrical Kadomtsev–Petviashvili equation," in *Nonlinear and Turbulent Processes in Physics: Proceedings of the 2nd International Workshop on Nonlinear and Turbulent Processes in Physics, Kiev, 1983* (Harwood Academic Publishers, Gordon and Breach, 1984), Vol. 2, pp. 1353–1360.

<sup>38</sup> J. W. Xia, Y. W. Zhao, and X. Lü, "Predictability, fast calculation and simulation for the interaction solutions to the cylindrical Kadomtsev–Petviashvili equation," *Commun. Nonlinear Sci. Numer. Simul.* **90**, 105260 (2020).

<sup>39</sup> M. Wang, J. Zhang, and X. Li, "Decay mode solutions to cylindrical KP equation," *Appl. Math. Lett.* **62**, 29–34 (2016).

<sup>40</sup> F. Calogero and A. Degasperis, "Solution by the spectral-transform method of a nonlinear evolution equation including as a special case the cylindrical KdV equation," *Lett. Nuovo Cimento* **23**, 150–154 (1978).

<sup>41</sup> F. Calogero and A. Degasperis, *Spectral Transform and Solitons: Tools to Solve and Investigate Nonlinear Evolution Equations* (North-Holland Publishing Co., Amsterdam, Holland, 1982).

- <sup>42</sup>A. Nakamura, "The Miura transform and the existence of an infinite number of conservation laws of the cylindrical KdV equation," *Phys. Lett. A* **82**(3), 111–112 (1981).
- <sup>43</sup>P. M. Santini, "Asymptotic behaviour (in  $t$ ) of solutions of the cylindrical KdV equation–I," *Nuovo Cimento A* **54**(2), 241–258 (1979).
- <sup>44</sup>P. M. Santini, "Asymptotic behaviour (in  $t$ ) of solutions of the cylindrical KdV equation–II," *Nuovo Cimento A* **57**(4), 387–396 (1980).
- <sup>45</sup>R. Hirota, *The Direct Method in Soliton Theory* (Cambridge University Press, 2004).
- <sup>46</sup>R. S. Johnson, "On the inverse scattering transform, the cylindrical Korteweg–de Vries equations and similarity solutions," *Phys. Lett. A* **72**, 197–199 (1979).
- <sup>47</sup>E. L. Ince, *Ordinary Differential Equations* (Dover, New York, 1944).
- <sup>48</sup>J. W. Miles, "On the second Painlevé transcendent," *Proc. R. Soc. Lond. A* **361**, 277–291 (1978).
- <sup>49</sup>W. Hu, J. Ren, and Y. Stepanyants, "Solitary waves and their interactions in the cylindrical Korteweg–de Vries equation," *Symmetry* **15**, 413 (2023).
- <sup>50</sup>L. A. Ostrovsky and E. N. Pelinovsky "Nonlinear evolution of tsunami-type waves," in *Theoretical and Experimental Investigation on the Tsunami Problem* (Nauka, Moscow, 1977), pp. 52–60 (in Russian).
- <sup>51</sup>K. Ko and H. H. Kuehl, "Cylindrical and spherical KdV solitary waves," *Phys. Fluids* **22**(7), 1343–1348 (1979).
- <sup>52</sup>J. W. Miles, "An axisymmetric Boussinesq wave," *J. Fluid Mech.* **84**(1), 181–191 (1978).
- <sup>53</sup>A. A. Lugovtsov, "Axially symmetric long waves on the surface of a varying-depth basin," *J. Appl. Mech. Tech. Phys.* **21**(6), 759–765 (1981).
- <sup>54</sup>Yu. A. Stepanyants, "Experimental investigation of cylindrically diverging solitons in an electric lattice," *Wave Motion* **3**, 335–341 (1981).
- <sup>55</sup>P. D. Weidman and R. Zakhem, "Cylindrical solitary waves," *J. Fluid Mech.* **191**, 557–573 (1988).
- <sup>56</sup>P. D. Weidman and M. G. Velarde, "Internal solitary waves," *Stud. Appl. Math.* **86**, 167–184 (1992).
- <sup>57</sup>J. M. McMillan and B. R. Sutherland, "The lifecycle of axisymmetric internal solitary waves," *Nonlinear Proc. Geophys.* **17**, 443–453 (2010).
- <sup>58</sup>K. Khusnutdinova and X. Zhang, "Nonlinear ring waves in a two-layer fluid," *Physica D* **333**, 208–221 (2016).
- <sup>59</sup>K. Khusnutdinova and X. Zhang, "Long ring waves in a stratified fluid over a shear flow," *J. Fluid Mech.* **794**, 17–44 (2016).
- <sup>60</sup>P. Fraunie and Y. Stepanyants, "Decay of cylindrical and spherical solitons in rotating media," *Phys. Lett. A* **293**(3–4), 166–172 (2002).
- <sup>61</sup>N. Hershkowitz and T. Romesser, "Observations of ion-acoustic cylindrical solitons," *Phys. Rev. Lett.* **32**(11), 581–583 (1974).
- <sup>62</sup>C. Ramirez, D. Renouard, and Yu. A. Stepanyants, "Propagation of cylindrical waves in a rotating fluid," *Fluid Dyn. Res.* **30**(3), 169–196 (2002).
- <sup>63</sup>E. Cumberbatch, "Spike solution for radially symmetric solitary waves," *Phys. Fluids* **21**(3), 374–376 (1978).
- <sup>64</sup>R. S. Johnson, "A note on an asymptotic solution of the cylindrical Korteweg–de Vries equation," *Wave Motion* **30**, 1–16 (1999).
- <sup>65</sup>P. D. Lax, "Integrals of nonlinear equations of evolution and solitary waves," *Commun. Pure Appl. Math.* **21**(5), 467–490 (1968).
- <sup>66</sup>J. C. Alexander, R. L. Pego, and R. L. Sachs, "On the transverse instability of solitary waves in the Kadomtsev–Petviashvili equation," *Phys. Lett. A* **226**, 187–192 (1997).
- <sup>67</sup>V. E. Zakharov, "Instability and nonlinear oscillations of solitons," *JETP Lett.* **22**, 172–173 (1975).
- <sup>68</sup>L. A. Ostrovskii and V. I. Shrira, "Instability and self-refraction of solitons," *Sov. Phys. JETP* **44**(4), 738–742 (1976).
- <sup>69</sup>V. I. Shrira and M. Z. Pesenson, "Soliton stability with respect to transverse perturbations of finite length and amplitude," in *Nonlinear and Turbulent Processes in Physics: Proceedings of the 2nd International Workshop on Nonlinear and Turbulent Processes in Physics, Kiev, 1983* (Harwood Academic Publishers, Gordon and Breach, 1984), Vol. 2, pp. 1061–1068.
- <sup>70</sup>D. E. Pelinovsky and Yu. A. Stepanyants, "Self-focusing instability of plane solitons and chains of two-dimensional solitons in positive-dispersion media," *JETP* **77**(4), 602–608 (1993).
- <sup>71</sup>J. Apel, L. A. Ostrovsky, Y. A. Stepanyants, and J. F. Lynch, "Internal solitons in the ocean and their effect on underwater sound," *J. Acoust. Soc. Am.* **121**(2), 695–722 (2007).